A New Model for Joint Shear Failure of Reinforced Concrete Interior Beam Column Joints

By

Hitoshi SHIOHARA*

(Received June 25, 1998)

The primary objective of this study is to point out an irrationality in the joint shear failure model, adopted by current design codes for reinforced concrete beam column joints. To investigate this issue, twenty tests of reinforced concrete interior beam column joints exhibiting joint shear failure are re-examined. Test data indicated that joint shear stress had increased in the most specimens, after joint shear failure initiated, while beam moment decreased due to a reduction in distance between stress resultants at the column face. The cause of the deterioration of story shear is identified to be a degrading of moment resistance of joint, originated from a finite upper limit of anchorage capacity of beam reinforcements through the joint core. A new mathematical model is introduced for joint shear failure to reflect this behavior. The behavior of the model is investigated and a new approach for the design of beam column joint in seismic zone is proposed on the basis of the proposed model.

Contents

* Associate Professor, Department of Architecture, Graduate School of Engineering, The University of Tokyo.

1. INTRODUCTION

The design of beam column joint is an important part of earthquake resistant design for reinforced concrete moment resisting frames. Beam column joints must provide sufficient stiffness and strength to resist and sustain the loads induced by adjacent beams and columns. Because high strength or large diameter steel bars are sometimes preferred in the design of building with smaller member size, the stress level in beam-column joints is increased. Designer must give careful consideration to this increased joint stress lest problems related to strength and/or stiffness result. For example, a strength lower than that based on full flexural strength of beams and columns may result. Furthermore, a reduction in stiffness due to premature formation of diagonal cracks and local crushing of concrete in the joint shear panel may also occur. These joint shear failures must be precluded to preserve the structural integrity of members jointed as rigid and strong as they are assumed in a structural analysis. To call attention to this issue an increasing number of building codes have recently developed provisions for the joint shear failure. Despite of the importance of the issue, no unified theory available for the provision have not been established.

The first part of this paper deals with the irrationality in the models for joint shear failure adopted in the most current design codes. The models are unanimously based on a hypothesis that the joint shear failure occurs when joint shear force reaches the shear capacity of the joint. This has not been confirmed by tests. To investigate this matter, twenty tests of reinforced concrete beam column joint exhibiting joint shear failune are reexamined. This paper then oultines the development a new model that move accurately portrays the mechanism of joint failure. Based on a parametric study using this model, a new approach for the design of interior beam column joints in seismic zones is proposed.

2. REVIEW OF DESIGN CONCEPT

In 1969, Hanson et al. reported test results of beam column joints and gave a quantitative definition of joint shear. They suggested that joint shear faiwre may be prevented by limiting the stress level lower than that at which joint shear failure occurs[1]. The ACI-ASCE 352 committee published in 1976 a proposal of beam column joint design, incorporating the provisions which limit joint shear stress[2]. Meinheit and Jirsa reported a series of joint tests designed to fail in joint shear so as to evaluate the joint shear capacity[3]. Based on these early developments, recent concrete codes, such as US [4] NZ [5] and Japan[6] adopted the design provision supplying limit value to joint shear stress. In recent years a significant number of tests of beam column joint have been carried out. The reliability of this design concept seems to be supported by those tests.

However, there still remains much ambiguity. No unified model or theory of the joint failure has not been established. Joint shear failure models of the ACI318-95[4], NZS3101[5] and AIJ guidelines[6] are different each other. In the AIJ guidelines, the joint shear failure is described as failure of diagonal concrete compressive strut in joint panel, whereas, NZS3101 assumes that tensile shear failure of truss mechanism defines for joint shear failure. Models portrayed in the codes are usually only qualitative ones. In addition, the limiting values for joint shear stresses is empirically derived.

3. DEFINITION OF JOINT SHEAR

The definition of joint shear V_j in Eq. (1) was introduced by Hanson et al.,[1] The joint shear V_j in Eq. (1) was defined as an internal force acting on the free body cut at the horizontal line at the mid height of the joint core as shown in Fig. 1. Physical meaning is very clear in this definition. The contribution of steel and concrete is taken into account separately. This paper adopted this definition for joint shear. Strain gage reading is necessary to monitor tensile force T and T'. An inelastic constitutive model of steel is also necessary when strain exceeds linearly elastic range.

$$V_j = T + C_s' + C_c' - V_c = T + T' - V_c = \Sigma a_t f_s + \Sigma a_t' f_s' - V_c \qquad (1)$$

where, C_s' : compressive force in steel bar, C_c': compressive force in concrete, T, T' : tensile force in steel, Σa_t , $\Sigma a_t'$: total sectional area of beam longitudinal reinforcement for positive moment and negative moment respectively, f_s , f_s' : tensile stress in beam longitudinal reinforcement, and V_c: column shear force (see Fig. 1). This definition is inadequate in determining the value of T or T' with great accuracy because the strain in parallel reinforcing bar usually do not indicate identical value. To measure the total force in the section, it is necessary to put strain gages on all longitudinal reinforcing bars. Although such an instrumentation is unrealistic for an ordinary test.

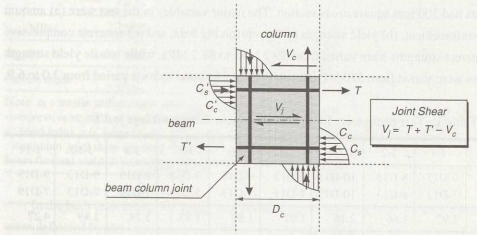

Fig. 1 : Definition of horizontal joint shear in R/C beam column joint

Because of the difficulty in evaluating the value of T and T' with reliability during test, joint shear reported in the literatures usually is assumming a constant value for j_b; the length of moment lever arm at the column face. Assuming no axial force in the beam, the moment at column face M_b is the product of T, and j_b. Hence Eq. (1) is rewritten as Eq. (2)

$$V_j = M_b / j_b + M_b' / j_b' - V_c \qquad (2)$$

The estimated joint shear obtained by Eq. (2) is suitable for statistical evaluation of test results found in the literature. However it is not suitable for defining the joint shear failure model, because V_j

obtained from Eq. (2) is not the real joint shear, but merely an index of the induced force level. For this reason the joint shear calculated from Eq. (2) is called hereafter the *pseudo joint shear* to distinguish the approximate nature of V_j obtained by Eq. (1). The most significant problem in using Eq. (2) is that the value of j_b changes during a test, due to the non-linearity of the material stress-strain relation and bond-slip relation. It is obvious that high compressive stress in concrete and poor bond give smaller values for j_b. Thus in this study the Eq. (1) is adopted to the joint shear force. The magnitude of forces is calculated from the measured strain, using strain gauges attached to the surface of the longitudinal steel bars. The change in joint shear force is of primary interest, rather than the absolute value.

4. REEVALUATION OF JOINT SHEAR TEST

Test results reported in two references [7,8] are re-examined using unpublished data. The whole test program is briefly summarized.

4. 1 Test Program

The specimens reported in reference[7] are listed in Table 1. Nine R/C 1/2.5 scale interior beam column joint subassemblages out of the eleven specimens tested were chosen because the other two specimens had transverse beam (J-3) or slab (J-9) . The beams were 240 mm wide and 300 mm deep, while the columns had 300 mm square cross section. The major variables in the test were (a) amount of longitudinal reinforcement, (b) yield strength of the reinforcing bars, and (c) concrete compressive strength. The concrete strengths were varied from 39.2 MPa to 81.2 MPa, while tensile yield strength of reinforcing bars were varied from 370 MPa to 1,456 MPa. The bond index μ varied from 3.0 to 6.9.

Table 1 : Test parameters for the beam column subassemblage test [7]

Specimen		J-1	J-2	J-4	J-5	J-6	J-7	J-8	J-10	J-11
Beam Bars	Top	9-D13	8-U13	10-D13	9-D13	9-D13	7-D13	9-D19	9-D13	9-D19
	Bot.	7-D13	8-U13	10-D13	7-D13	7-D13	5-D13	7-D19	7-D13	7-D19
ρ_t (%)	Top	1.92	1.66	2.16	1.92	1.89	1.43	3.24	1.89	4.27
	Bot.	1.44	1.66	2.16	1.44	1.43	0.98	4.27	1.43	3.24
f_y (MPa)		638	1 456	515	839	676		370	700	372
σ_B (MPa)		81.2		72.8		79.2			39.2	
μ		3.0	6.9	2.6	4.2	3.2	3.2	2.6	4.7	3.7
v_{pu} (MPa)		14.2	15.3	14.5	16.3	15.1	12.0	17.1	10.8	12.7
R_u (%)		2.7	2.8	3.1	3.0	2.9	3.0	1.8	1.9	2.0
Failure mode		BJ	J	BJ	BJ	BJ	BJ	BJ	J	J

Note ρ_t : tensile reinforcement ratio, f_y : yield point strength, σ_B : concrete compressive strength, μ: bond index = $(f_y/\sqrt{\sigma_B})(d_B/D_c)$ (f_y and σ_B in MPa), d_B : nominal diameter of beam bar, D_c : column depth, v_{pu} : maximum joint shear obtained from Eq. (2). R_u : story drift at maximum story shear, BJ : joint shear failure after beam flexural yield, J: joint shear failure without beam flexulal yield.

Table 2 lists the eleven specimens tested by Teraoka[8]. The sizes of the beam and column sections are the same as the specimens in the reference[7]. The major variables in teraoka's tests were (a) concrete strength, including the effect of light weight concrete, and (b) the amount of joint hoops. Concrete strength varies from 30.5 MPa to 46.7 MPa. The amount of joint hoop ratio varied from 0.6% to 1.8%.

Table 2 : Test parameters for the beam column subassemblage test [8]

Specimen		No.1	No.2	No.3	No.4	No.5	No.6	No.7	No.8	No.9	No.10	No.11	No.12
Beam Bars	Top	2-D22 & 2-D19			4-D22					2-D22&2-D19		4-D22	
	Bot.	2-D22 & 2-D19			4-D22					2-D22&2-D19		4-D22	
ρ_t (%)	Top	2.16			2.48					2.16		2.48	
	Bot.	2.16			2.48					2.16		2.48	
f_y (MPa)		411 (D22) 406 (D19)			411					411 369		396	
ρ_h(%)		1.2	1.8	1.2	1.2	1.8	1.2	1.2	1.8	0.6	1.2	0.6	1.2
σ_B (MPa)		33.6 (LC)		34.5	36.6		39.6 (SF)	46.7		30.5 (LC)		32.2	
μ		5.2 4.5	5.2 4.5	5.2 4.4	5.0	5.0	4.8	4.5	4.5	5.5 4.3	5.5 4.3	5.2	5.2
v_{pu} (MPa)		10.5	10.1	11.1	12.3	12.4	12.8	13.1	13.2	9.4	9.2	10.3	10.6
R_u (%)		2.0	2.0	2.0	2.0	2.0	2.0	2.0	2.0	2.0	2.0	2.0	2.0
Failure mode		J	J	J	J	J	BJ	BJ	BJ	J	J	J	J

Note ρ_t : tensile reinforcement ratio, f_y : yield point strength, ρ_h: joint hoop reinforcement ratio, σ_B : concrete compressive strength of joint,in which LC and SF mean light weight concrete and steel fibre concrete respectively, μ: bond index = $(f_y/\sqrt{\sigma_B})(d_B/D_c)$ (f_y and σ_B in MPa), d_B : nominal diameter of beam bar, D_c : column depth, v_{pu} : maximum joint shear obtained from Eq. (2). R_u : story drift at maximum story shear, BJ : joint shear failure after beam flexural yield, J: joint shear failure without beam flexulal yield.

In the both tests series, the upper and lower columns were supported by pin joints. The beam ends were deflected by the same amplitude, but in the opposite directions. The specimens were subjected to reversed cyclic load with increasing amplitude to failure. Strains of longitudinal reinforcing bars were monitored by strain gauges attached on the surface of the bars. Observed failure mode was joint shear failure (J or BJ) before or after beam flexural yielding.

4. 2 *Story Shear*

The envelope curves of story drift and story shear relation are compared in Figs. 2 and 3. In all the specimens, the degradation of story shear started at story drift larger than 2 to 3%.

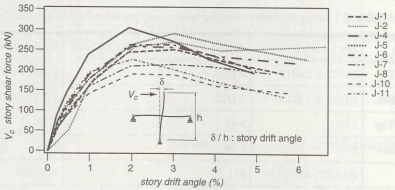

Fig. 2 : Relation of story shear to story drift[7]

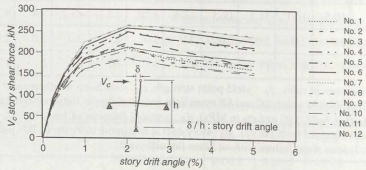

Fig. 3 : Relation of story shear to story drift[8]

4. 3 *Nonlinear Constitutive Model for Steel*

A nonlinear constitutive model for cyclic loading was used to evaluate the stress from the strain of the longitudinal reinforcing steel in beams. The Ramberg-Osgood curve was incorporated to the model with a linearly elastic stage and yield plateau. Tensile test results of reinforcing bars under monotonically increasing load were used to determine the skeleton curve. A typical hysteresis curve calculated by the model is shown in Fig. 4.

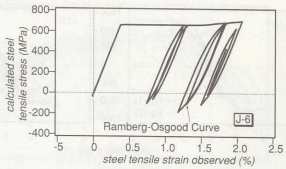

Fig. 4 : Example of stress-strain relation predicted using Ramberg-Osgood model

4. 4 *Stress in Flexure Reinforcement at Column Face and Joint Shear*

The steel stress in tensile reinforcement of a beam in the outer layer at the column face are plotted against story drift for specimens J-2, J-7 and J-10 in Fig. 5. Although the story shear decreased due to cyclic loading in these three specimens as demonstrated in Fig. 2, the tensile stress increased at load peaks.

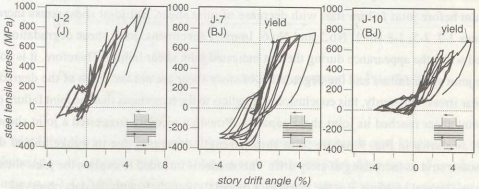

Fig. 5 : Typical relation of story drift and tensile stress in first outer tensile reinforcement

Joint shear V_j was calculated using Eq. (1) in the following section, assuming the stress in all bars including bars, without strain gauges, is identical. All specimens had the strain gages in the outer layer reinforcing bars, while only the specimens from J-6 to J-11 had strain gauges in the inner layer reinforcing bars. The strain in the inner layer bars of the specimens J-1 to J-5 was calculated from outer bar strain reading using the Bernouli's assumption that plain section remains plain.

Joint shear forces are calculated using the steel stresses. The results are shown in Fig. 6. The joint shear increased with story drift, whereas joint shear calculated by Eq. (2) plotted with dotted line in Fig. 3 showed strength degradation. The joint shear by Eq. (2) were calculated from beam moment by assuming distance of stress resultants to be 7/8 of the effective depth. The joint shear evaluated by Eq. (1) is smaller than that evaluated by Eq. (2) when story drift is small. When the story drift angle exceeded 2%, the value evaluated by Eq. (1) became larger than that evaluated by Eq. (2).

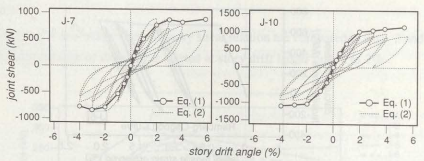

Fig. 6 : Story shear and joint shear relation using different definition of joint shear

4. 5 Joint Shear Stress

Joint shear stresses of twenty specimens were evaluated by Eq. (1) at peak loads of each leading cycle and are plotted against story drift angle in Figs. 7 and 8. Joint shear stress was calculated for the effective joint sectional area defined as a product of column depth and effective joint width suggested in AIJ guideline[7]. Joint shear stress was normalized by the square root of concrete compressive strength. Contrary to Figs. 2 and 3, the shear stress did not degrade with deformation except for specimens J-11, No. 8 and No. 11. If compressive failure of diagonal strut occurred, joint shear stress should reach maximum before joint failure start with decrease of joint shear. But joint shear stress increased in specimens J-2, J-5, J-8 No.1, No.2 and No.6. In most specimens, joint shear degradation was not observed while the appearance during the test indicated joint shear failure. Therefore, it is concluded that the joint shear failure and the degradation of story shear are not the result of the degradation of joint shear stress. Obviously, this conclusion contradicts to the hypothesis that the joint failure occurred when joint shear reached its joint shear capacity. Priestley recently suggested a joint shear failure model[9] as shown in Fig. 9, where joint shear strength decreases due to weakening of diagonal compressive strut as increasing of story drift. This model is intended to explain the joint shear failure after beam flexural yielding. But the Priestley's model[9] contradicts with the data observed.

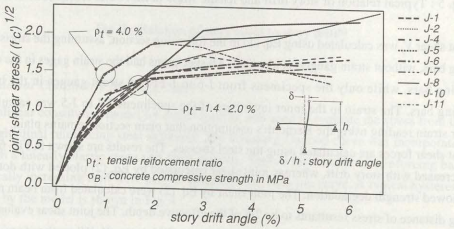

Fig. 7 : Relation of story shear and joint shear evaluated with Eq. (1) at peaks load[7]

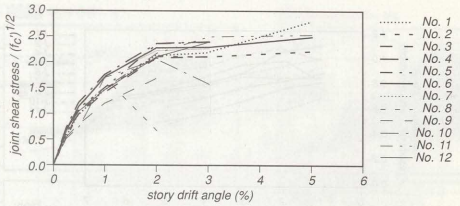

Fig. 8 : Relation of story shear and joint shear evaluated with Eq. (1) at peaks load[8]

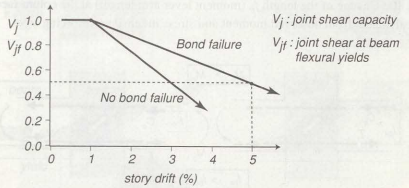

Fig. 9 : Model for joint shear degradation proposed by Priestley[9]

It is noted that the joint shear stress of those with ordinary strength steel longitudinal bars with high volume (ρ_t = 4%) showed high joint shear stress, while the joint shear stress of specimens with low volume (ρ_t = 1.4 - 2.0%) apparently have lower joint shear stress. This fact suggests that attained joint shear level are function of amount of longitudinal steel as well as concrete compressive strength. On the contrary, the amount of joint hoop seems to be have less effect on the attained joint shear as shown in Fig. 8, in which specimens with different amount of joint hoop are included.

4. 6 Shift of the Location of Stress Resultants

In order to show that the story shear degradation at a large story drift is attributed to the movement of the location of the stress resultants at the column face, Fig. 10 shows the change in the distance j_b of stress resultants at peaks load. The value of j_b were calculated using the relation that the moment at the column face is product of force in tensile longitudinal reinforcement and j_b. In all the specimen, the j_b decreased as story drift increased. Hence, the decrease of story shear is caused by the degradation of moment resistance, which occurred due to the reduction of the distance of stress resultants.

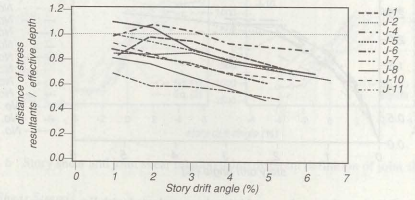

Fig. 10 : Change of the length j_b (moment lever arm length) at the colum face calculated from observed moment and stress in tensile reinforcing steel

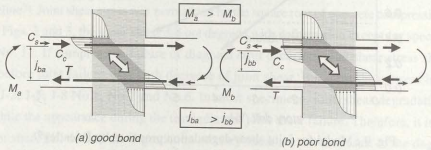

Fig. 11 : Effect of poor bond on moment resistance of beam column joint

4. 7 *Change of Stress in Compressive Reinforcement*

Decrease of distance between locations of stress resultants were partly because the location of compressive stress resultants shifted to the center of beam. It is attributed the expansion of concrete compressive zone for flexural resistance. But the most significant reason is the change of stress in compressive reinforcement from compression to tension. These changes are activated by the anchorage softening; yield or degradation of anchorage capacity, of beam reinforcement through the joint core as well as volume expansion in horizontal direction due to crack opening of joint panel. The sequence of beam moment reduction due to poor anchorage is depicted in Fig. 11. The observed distribution of tensile stress along the longitudinal bar through joint core are plotted for the specimens J-7, J-10 and J-11 in Fig. 12.

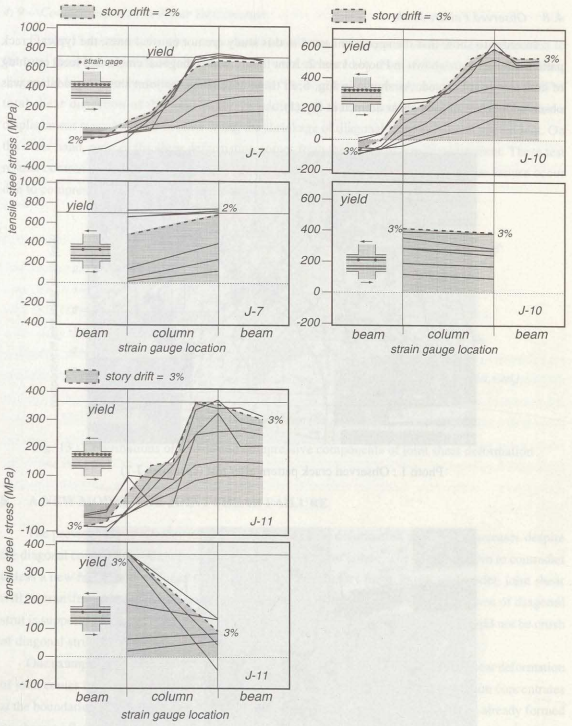

Fig. 12 : Observed stress in beam longitudinal reinforcements

As shown in Fig. 12, the compressive reinforcement have tensile stress. It is noted that the tensile stress in steel bars in the second layer is much larger than that of the first layer. Therefore, it is presumed that one of the fundamental cause of the degradation of story shear is the upper limit of anchorage capacity, not the joint shear capacity degradation.

4. 8 *Observed Failure Mode*

In order to show that the specimens used in this study are not unusual ones, the typical crack pattern after tests are shown in Photos 1 and 2. Joint failure with a diagonal cracks and local crushing of concrete are observed. As shown in Fig. 6, in these specimens, no joint shear degradation was observed in terms of joint shear defined in Eq. (1).

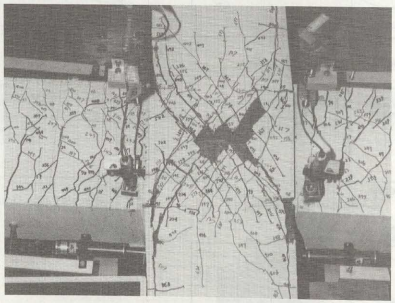

Photo 1 : Observed crack pattern after test (specimen J-7)

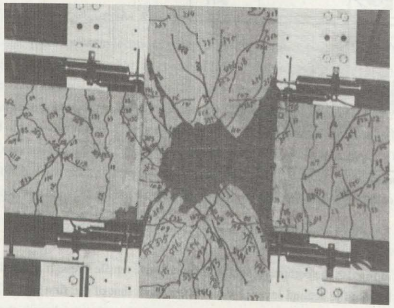

Photo 2 : Observed crack pattern after test (specimen J-10)

4. 9 *Components of Joint Shear Deformation*

Figure 13 compares the two components; contribution of diagonal compression and tension to the total shear deformation of joint panel. They were measured by a set of displacement transducers, diagonally located on the surface of the specimen. The compressive component is smaller than 20% of total shear distortion of the joint panel. In addition to that, no sudden increase of compressive displacement was observed. In other word, the shrinkage of diagonal concrete strut is not evident. On the other hand, most of the shear deformation comes from the diagonal tensile component. These test results contradict the model of Japanese design guidelines[6] which assume joint shear failure occur due to compressive failure of diagonal compressive strut.

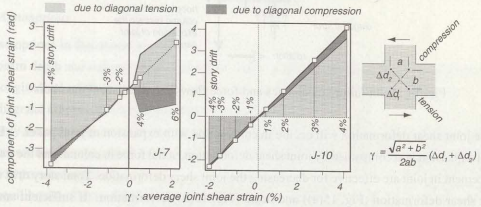

Fig. 13 : Contributions of tensile and compressive components of joint shear deformation

5. A NEW MODEL FOR JOINT SHEAR FAILURE

The previous section demonstrated that the joint shear deformation apparently increases despite the diagonal concrete strut showes no evidence of compressive failure. The two facts seem to contradict unless a new model is introduced to reconcile the contradictory facts. In the new model, joint shear will be transferred by diagonal strut like the traditional strut model, because existence of diagonal strut is supported by tests and analyses. However, cause of joint shear deformation should not be crush of diagonal strut due to compressive force in strut.

One example of model which satisfy the above condition is shown in Fig. 14. The shear deformation of joint comes from rotational movement of four rigid segments. Thus shear deformation concentrates at the boundaries which consists of diagonal cracks and flexural cracks, which had been already formed by shear or flexural stress in previous cyclic loading as depicted in Fig. 14. Usually beam column joint have such cracks except some special case such as a beam column joint with debonded beam bars. In the model, the rigid segments rotates around contact points, the movement of which will be detected by an instrumentation as joint shear deformation during tests. In reality, the rigid segments are not perfectly rigid. Thus the contact point of the segments is a finite size.

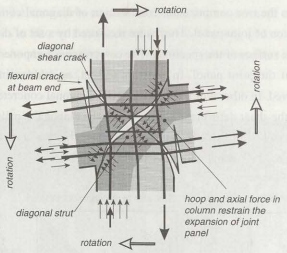

Fig. 14 : Joint failure mechanics and force flow among adjacent members

The joint shear deformation will occure in conjunction with expansion of joint panel. Because the joint expansion is accompanied by joint shear deformation, axial force in column and the transverse reinforcement in joint are effective for decreasing the joint shear deformation. Total story drift consists of joint shear deformation (Fig. 15(a)) and beam (Fig. 15(b)) deformation. If sufficient amount of hoops are provided, the opening of the diagonal cracks is restrained, which keeps the joint stiffness high, and the percentage of beam deformation occupying in the total story drift increase, because the springs for two deformation modes are coupled in serial. In this case, the failure mode of joint becomes beam yielding.

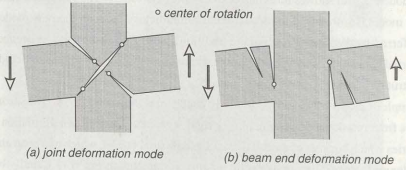

Fig. 15 : Joint failure mechanics model

5. 1 Moment and Shear Resistance of the Connection

Because a beam column joint resists moment as well as joint shear, two mechanism of joint failure should be identified, i.e. (1) failure of moment resisting system and (2) failure of shear resisting

system. As discussed in previous section, most of the joint shear failure of beam column joint were failure of moment resisting system. So the model shown in Fig. 14 are simplified to be suitable for mathematical model where it assumes simple 45 degree cracks, which divide the joint panel into four triangular segments. By using this model, the moment resisting system of beam column joint is investigated. In order to resist to the relative movements at the boundary of the segments, internal stress arises in longitudinal steel, joint hoops and concrete to resist the rotation of the segments. The location and distribution of boundary stress in concrete is assumed as shown in Fig. 16 with consideration of compatibility of displacement and strain due to rotation of the segments. The whole structural system including beam and column, and applied external forces on the beam-to-column joint subassembly is defined in Fig. 17.

5. 2 Assumptions

The assumptions in this model are;

a) beam depth and column depth is identical and it is the unit of length use in this analysis.
b) longitudinal reinforcements resist only to the axial force and no dowel force occur.
c) diagonal cracks exist with inclination of 45 degree.
d) only normal stress is transmitted across the concrete cracks and distribution of the normal stress is assumed as a rectangular stress block, where the concrete stress is equal to the concrete compressive stress σ_c .
e) equilibrium of external force and internal force are considered, whereas, the compatibility of deformation is not necessarily satisfied.
f) location and magnitude of the external forces acted on the beam-column-connection substructure is symmetric in both vertical and horizontal direction.

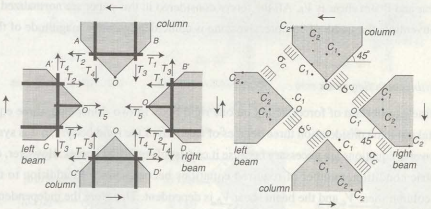

Fig. 16 : Internal forces and their notations

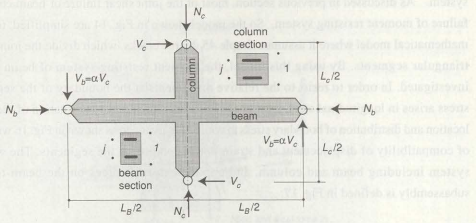

Fig. 17 : Geometry of beam-column joint and external forces

The parameter to describe the problem, geometry and the dimensions, the external force, and the boundary stresses need to be defined. In this paper, the following notations are used, j: distance between tensile reinforcement and compressive reinforcement on the cross section of beam and column to depth of beam, t : thickness of beam-to-column joint panel, N_c : column axial force divided by $t\sigma_c$, $t\sigma_c$: the product of joint sectional area, and concrete compressive stress, N_b: beam axial force divided by $t\sigma_c$, L_B : the length of beam L_c : the length of column and α : L_c/L_B.

Unknown variables describing the set of the internal forces are also introduced. The tensile forces T_1, T_2, T_3, T_4, T_5 (positive in tension) in reinforcement are shown in Fig. 16(a), where, tensile force T_5 in distributed hoop in height direction assumed to concentrate at the mid height. The compressive force C_1, C_2 (positive in compression) in concrete are shown in Fig. 16(b). They are considering the x and y component of forces acting perpendicular to the segment boundary. Column shear V_c is identical to story shear and Beam shear is V_b. All the forces considered in this paper are normalized by $t\sigma_c$. By this unit convention, the width of compressive zone is coincident with the magnitude of the concrete forces.

5. 3 *Equilibrium in Segments*

To define equilibrium of forces acting on one rigid body in two-dimension, three equations are necessary, taking into consideration three degrees of freedom of the rigid body. In this system shown in Fig. 16, twelve equations are necessary because it consist of four rigid bodies. However, considering the symmetric condition, number of required equations becomes six. In addition to that, in this system the column shear V_c and the beam shear V_b is dependent. Therefore the independent equations to represent the equilibrium is estimated to be five. They are as follows.

The equilibrium of x and y directional forces on the right beam are expressed as,

$$-T_1 - T_2 - T_5 + C_1 + C_2 - N_b = 0 \tag{3}$$

$$T_3 - T_4 + C_2 - C_1 + \alpha V_c = 0 \tag{4}$$

respectively. The equilibrium of moment with respect to the center point O on the right beam is given.

$$\frac{L_B}{2}\alpha V_c + \frac{1}{2} j\,(T_3 - T_4) + j\,(T_1 - T_2) + C_2\,(1 - C_2) - C_1 C_1 = 0 \tag{5}$$

The equilibrium of x and y directional forces on the right top column is,

$$T_1 - T_2 + C_2 - C_1 + V_c = 0 \tag{6}$$

$$-T_3 - T_4 + C_1 + C_2 - N_c = 0 \tag{7}$$

respectively. The set of simultaneous equations of second order from Eqs. (3) to (7) gives solution to five unknown variables, provided other variables are confirmed.

5. 4 *Comparison of Test and Analysis*

The new model and its equations of equilibrium are applied to the test results to check the reliability of model. Test data were used for T_1 T_2 and T_5, while the unknown valuables T_3 and T_4, the concrete stress C_1 and C_2, and Column Shear V_c were calculated by solving the set of equations. The value for tensile stress T_5 is assumed to be equal to the total yield strength of hoop, based on the description of strain in hoops in the reference[7]. The concrete compressive stress σ_c was assumed to be 85% of concrete compressive strength. Fig. 18 show the calculated forces acting on the right beam segment, as well as comparison with the stress in column steel and column shear observed in the test. To get the solutions for the simultaneous equation, Maple V; a software package for symbolic mathematical tool, and its solve function is used.

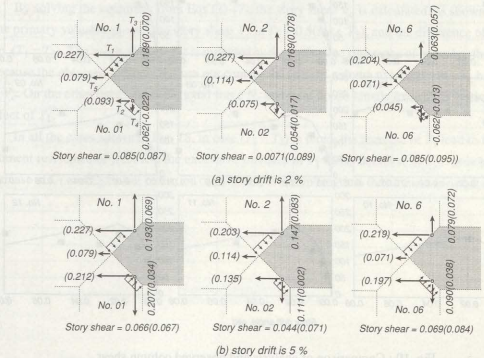

Fig. 18 : Predicted column shear by the model (number in parentheses is observed value)

In the specimen No. 1, calculated values for column shear V_c shows good correlation, while the forces T_4 and T_5 in column rebars do not show good correlation. It is partly because, the column section have multi layered longitudinal bars, which is different from the model, where only one layer of steel is assumed. In the specimens No.2 and No.6, predicted V_c underestimate the test value in particular in the case where, tensile force in compressive bars is very large value.

In the Fig. 19, the calculated column shear V_c are plotted against the test result. In this calculation, the force in joint hoops T_5 is assumed zero due to lack of the data of strain history for hoops, while the stress in the hoops increase according to the joint shear deformation. As the result of the neglects, the calculated shear V_c is smaller than test results in all the specimens. The degradation of story shear after the maximum column attained at about 2% of story drift is show good correlation, except at very large story drift such as 6% or more. The unreliable measurement of strain history may be attributed to the discrepancy.

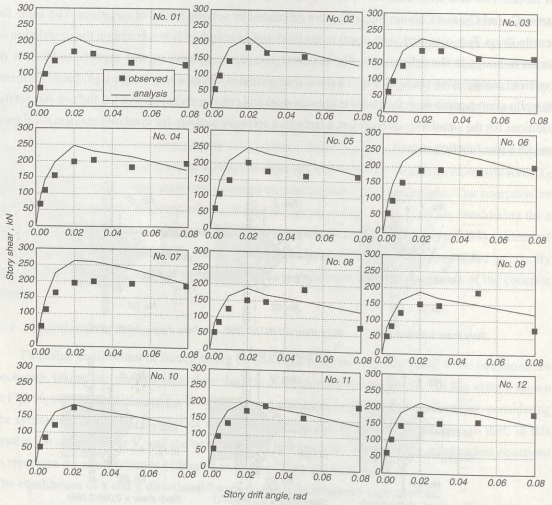

Fig. 19 : Comparison of analysis and observed column shear

6. PARAMETRIC STUDY

6. 1 *Parameters*

A parametric study was carried out using the model discussed in the previous section. The varying parameters include (a) the size of beam and (b) ratio of column length to beam length. Table 3 lists the parameters.

Table 3 : Parameters for a parametric study

parameters	Case 1	Case 2	Case 3
length of beam L_B	10	8.33	10
length of column $L_c = \alpha L$	5	4.17	20
α (= L_C/L_B)	0.5	0.5	2.0

The value of j; distance of stress resultant in beam is assumed to be 80% of column depth for all the cases. The case 2 represents the connection, where the size of beam is 20% larger than case 1. By comparing the case 1 and case 2, the effect of section size could be evaluated. The case 3 represents the connection with longer column. By comparing the case 1 and case 3, the effect of column shear could be examined. In this parametric study, V_c T_3 T_4 C_1 and C_2 are chosen as an unknown variables, whereas, the T_1 T_2 and T_5 are given.

6. 2 *Story Shear Capacity*

By solving the equations from Eqs.(3)-(7), the story shear V_c is calculated. as shown in Fig. 18. The primary valuable govern the story shear V_c is $T_1 + 0.5(N_b + T_5)$, and the difference of T_2 and T_1, i. e. $(T_1 - T_2)$. The value of $(T_1 - T_2)$ is regarded as the anchorage resistance of beam bar through joint. Because the obtained solution V_c does not contain the term of column axial force N_c, N_c has no effect of V_c. On the other hand, the beam axial force N_c and joint hoops tensile force T_5 is equivalent to the effect of T_1.

In all the cases shown in Fig. 18, in case $(T_1 - T_2)$ is fixed, the increase of T_1 lead to increase the moment resistance of joint and the excessive increase of T_1 cause decrease of V_c. It is because, the increase of C_1 and C_2 causes reduction of moment lever arm length in the moment resistant mechanism.

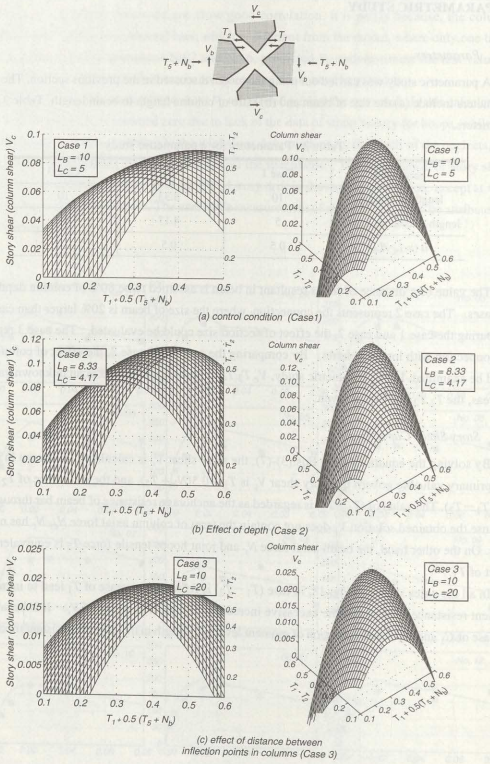

Fig. 20 : Example solution for story shear V_c calculated by the new model

Maximum column shear exist for each $(T_1 - T_2)$ value. It means that provided the amount of the beam tensile reinforcement is too large, story shear will attain maximum load before the beam rebar yield. Thus the peak value is interpreted as a capacity of the moment resistance of joint. The peak values are larger if the anchorage $(T_1 - T_2)$ resistance is larger. This model clearly explain that the maximum moment resistant capacity of joint really exists, and the moment resisting capacity depends on the anchorage capacity of beam bar through joint. It is also noted that this model does not assume any compressive failure of diagonal concrete strut.

By comparison of the solution for the case 1 the case 2 and the case 3, it is recognized that story shear capacity is also the function of member depth d, and distance between inflection point in column. Twenty percent increase of the depth lead to the approximately 20% increase of story shear capacity. (Fig. 20(b)) and four times longer distance between inflection point in column lead to about one fourth of story shear capacity (Fig. 20(c)).

6. 3 *Pseudo Joint Shear at Moment Capacity of Beam Column Joint*

As stated in the previous sections, investigated test data of the joint shear stress defined by Eq. (1) showed that joint shear did not decrease in the most specimen, while moment resistance of joints degraded. However the most reported joint shear stress is not by Eq(1), but is pseudo joint shear stress calculated by Eq. (2). By using the same notation used for Eq. (3) to (7), Eq. (2) is modified to an equivalent Eq. (8), in which, the relation of column shear V_c and joint shear V_j is defined.

$$V_j = \left\{ \frac{\alpha\,(L_B - 1)}{j} - 1 \right\} V_c \tag{8}$$

Figure 21 shows the pseudo joint shear V_j calculated for the model listed in Table 3. In this caluculation the value for j is assmued to be 0.8. As recognized in Eq. (8), the pseudo joint shear is proportional to the column shear V_c. Therefore, the calculated joint shear shows similar tendency as story shear shown in Fig. 21.

It is observed in these three cases, that the maximum joint shear range from 0.3 to 0.4 in common. Hence the predicted capacities in terms of pseudo shear stress is close to each other, despite the structural parameters are different in these three cases.

Amount of joint hoops is considered not to have significant effect to increase the joint shear capacity. So the amount of hoops is not taken into account in estimating the joint shear capacity in AIJ guidelines[6]. The prediction of the new model support this fact as shown in Fig. 21.

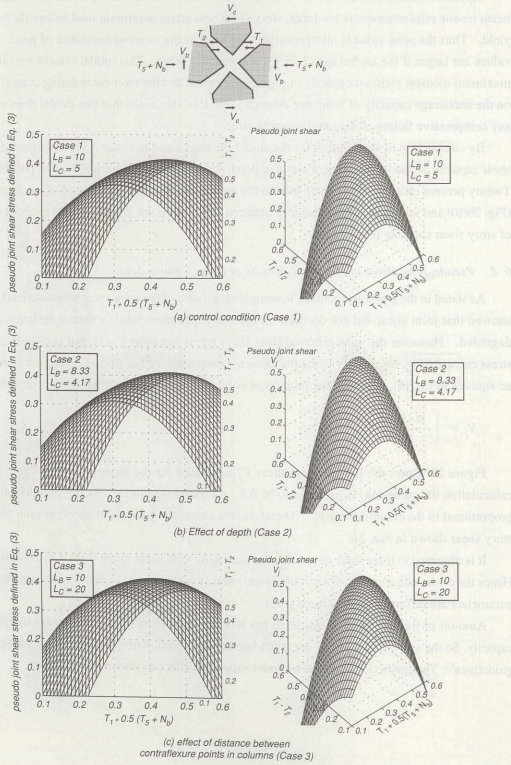

Fig. 21 : Example solution for pseudo joint shear calculated by the new model

7. DISCUSSION

7. 1 Beam Column Joint Designed by the Current Code

Although the existing design methods[5, 6, 7] set limit value for the induced joint shear stress so as to prevent joint shear failure, this method have been effective empirically. It is partly because by the limiting the joint shear stress, the amount of beam reinforcement is restricted as well as the ratio of diamiter of the bar is restricted. As a result bond stress is usually kept lower as a side effect. Thus, the anchorage capacity is sufficient. This is one reason because the design provisions in current codes seem to work properly despite of their irrational model for joint shear failure.

But another issue could be identified on the model considering compressive failure of diagonal strut explaining the joint shear failure. There is few test reported in references that the column did not sustain constant axial load after the joint failure. The exceptions is only one specimen reported by Kimura in 1997, where a exterior joint panel was crushed under combination of joint shear and extremely high axial force level in column with approximately 60% of concrete compressive strength, in which resistance to the axial load diminished. Maybe this specimen was exceptional case, in which diagonal strut in joint actually crushed. Because the diagonal strut formed in joint panel is on the path of axial force in beam column joint, strut compressive failure should cause the loss of axial force resistance. Therefore, in the most cases, observed joint shear failure is not associated with strut compressive failure, but the expansion of diagonal cracks.

It is concluded from the discussion above that the design based on the limiting of joint shear capacity is effective if it is applied to beam column joint with conventional reinforcing detail, while it have no rational basis. If the design is applied to special reinforcing detail or special configuration of joint, such as prestress concrete beam column joint, the current design may be conservative for one joint, while it is dangerous for another joint. Therefore it is recommend to reexamine the test of joint shear failure based on the real stress in the longitudinal reinforcement to develope more rational model for joint shear failure.

7. 2 Implication of the New Model for Design of Beam Column Joint

The new model for a moment resisting capacity of beam column joint leads to a new approach for the design for joint shear failure. To prevent the joint failure of beam column joint designed for weak beam-strong column philosophy, it is effective to increase the moment capacity of joint relative to the induced moment at beam ends which yield in flexure. However, in conventional reinforcement detail, increasing of longitudinal reinforcement in joint core inevitably also increase the beam moment capacity because the longitudinal reinforcement for joint and beam is common. The method to overcome the problem is to arrange aditional longitudinal bar only in joint panel and joint hoops to make joint moment capacity larger than that of beams using reinforcing detail as shown in Fig. 22(a). By the additional reinforcement in the joint, joint deformation depicted by Fig. 15(a) will be significantly diminished, while the beam deformation in Fig. 15(b) will be increased. However no experimental works on this kind of special reinforcement in beam column joint have not been reported before. By

this countermeasure, failure mode of joint is presumed to be changed to more favorable ductile failure mode by preventing the plastic deformation concentrated in joint shear panel. So the change of failure mode will be easily achieved, not by reducing the joint shear.

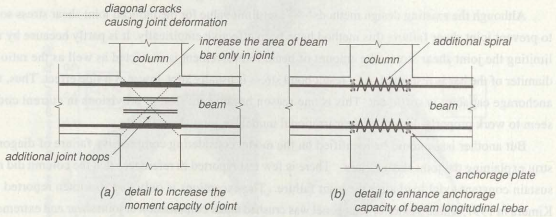

Fig. 22 : Probable reinforcing detail to prevent joint shear failure

Although the proposed reinforcing method may be effective to get favorable failure mode, it will be less effective increasing absolute moment joint capacity, because poor anchorage of beam reinforcement going through the joint makes moment resisting capacity lower, as predicted by the new model shown in Fig. 20. It is in particular important for the design of beam column joint after the beams yielding. Cyclic reversal loading after beam yield imposes high demand for anchorage capacity, which accelerate deterioration of anchorage due to bond. It sometimes causes joint shear failure after beam yield and it is well known fact. To prevent the deterioration of the moment capacity of the joint, some special mechanical anchorage device or spiral will be effective as shown in Fig. 22(b).

8. CONCLUSION

The joint shear input of twenty interior beam column joint, which showed failure mode of joint shear, subjected to cyclic loading simulating earthquake load are investigated. It is concluded as follows;

1. In the specimens failed in joint shear in the tests, joint shear force did not degrade for the most specimens, although the story shear degraded due to cyclic load.

2. The cause of the degradation of story shear was attributed to the finite upper limit of anchorage capacity of beam longitudinal reinforcement through the joint. It makes the tensile stress in compressive reinforcement shift to tension. The lost compressive resistance of the compressive force also causes the location of stress resultant of compression shift to the mid-height of the section. As a result, the moment resistance of beam decreased.

3. For a significant number of joint shear failure specimens, joint shear failures may not be a compressive failure of diagonal concrete strut as assumed in some current design code. It is rather the joint shear failure occurred due to expansion of diagonal cracks. In other word, the direct relation between joint shear input and joint shear deformation does not exist in those specimens.

4. Quite a large number of experiments on joint shear failure have been accumulated, while the joint shear data based on the stress in the longitudinal reinforcement are scarce. More investigation of test data is urged to derive more reliable general conclusion.

5. The hypothesis of joint shear failure which assumes that the joint shear failure is the result of diagonal compressive failure of joint panel does not have rational basis as far as the observed test data concerns.

Based on the examination of tests, the necessity of a mathematical model which accounts the mechanism of moment resistance of joint panel was emphasized. To explain the behavior of joint failure, a new model was proposed, which consists of divided segments by diagonal cracks in joint shear panel. They rotates due to bending moment from beams and columns. The equilibrium of internal stress in steel and concrete at the boundary and external forces acting on beam ends and column ends is taken into account to predict the moment resisting capacity of joint shear panel. It is concluded from the analysis using the model.

6. The reliability of the model and its assumptions were verified. The prediction of model showed good correlation with the effects of parameters including the concrete compressive strength, amount of beam reinforcement, and amount of joint hoop.

7. The prediction of behavior of the new model for the moment resisting capacity of beam column joint leads to a new approach to prevent from joint shear failure. To modify the joint failure into more ductile beam yield failure mode, it is effective to increase the moment capacity of joint, relative to the induced moment at beam ends yielding in flexure, but joint shear resisting capacity.

Acknowledgement

Dr. M. Teraoka, senior researcher of Fujita Corp. is greatly acknowledged for his offering of detailed test data including strain history obtained in his research project. The assistance by Mr. F. Kusuhara and Mr. S. Kishikawa, graduate students, Graduate School of Engineering, the University of Tokyo, is sincerely appreciated on test data reduction and some drawings used in this paper.

References

1) Norman W. Hanson, and Harold W. Connor : Seismic Resistance of Reinforced Concrete Beam-Column Joint, Journal of the Structural Division, ASCE, Vol. 93, No.ST5, Oct. 1967, pp. 533-560.
2) ACI-ASCE Committee 352 : Recommendations for Design of Beam-Column Joints in Monolithic Reinforced Concrete Structures, ACI Journal, No. 73-28, July 1976, pp. 375-387.

3) Donald F. Meinheit, and James O. Jirsa : Shear Strength of R/C Beam-Column Connections, Journal of the Structural Division, ASCE, Vol. 107, No. ST11, Nov. 1981, pp. 2227-2244.

4) ACI 318-95: *Building Code Requirements for Structural Concrete and Commentary*, ACI, Farmington Hills, Michigan, pp. 367.

5) Standards New Zealand: *NZS3101Concrete Structures Standard :Part 1 - The Design of Concrete Structure:1995*, 1995.

6) Architectural Institute of Japan : *AIJ Structural Design Guidelines for Reinforced Concrete Buildings*, Tokyo, 1994, 168 pp..

7) Koji Oka and Hitoshi Shiohara : Tests of high-strength concrete interior beam-to-column joint subassemblages, Proceedings of the Tenth World Conference on Earthquake Engineering, Balcelona, 1992, pp. 3211-3217.

8) Masaru Teraoka : A study on seismic design of R/C beam-to-column joint in high rise frame structure, Research Report of Fujita Institute of Technology, Extra Issue No. 5, 1997, (in Japanese).

9) M. J. N. Priestley : Displacement-Based Seismic Assessment of Existing Reinforced Concrete Building, Proceedings of the Pacific Conference on Earthquake Engineering, Volume 3, Australia, 20-22 November, 1995, pp. 225-244.

10) Kashiwazaki, T., T. Nagai and H. Noguchi : Parametric Study on the Shear Strength of R/C Interior Beam-Column Joints using Finite Element Method, Transactions of Japan Concrete Institute, Vol. 18, 1996, pp. 275-282.

11) Hideki Kimura, Taku Kawai, Masayuki Iwata and Tokio Watai, Experimental Study on Behavior of R/C External Beam-to-Column Joint under High Axial Load, Transactions of AIJ Annual Meeting, Vol. C-2, September 1997, pp. 389-390 (in Japanese)